

Generalized Causal Set d'Alembertians

Siavash Aslanbeigi,^{a,b} Mehdi Saravani^{a,b} and Rafael D. Sorkin^{a,b,c,d}

^a*Perimeter Institute for Theoretical Physics, 31 Caroline St. N., Waterloo, ON, N2L 2Y5, Canada*

^b*Department of Physics and Astronomy, University of Waterloo, Waterloo, ON, N2L 3G1, Canada*

^c*Department of Physics, Syracuse University, Syracuse, NY 13244-1130, U.S.A.*

^d*Raman Research Institute, C.V.Raman Avenue, Sadashivanagar, Bangalore 560 080, India*

E-mail: msaravani@perimeterinstitute.ca,

saslanbeigi@perimeterinstitute.ca, rsorkin@perimeterinstitute.ca

ABSTRACT: We introduce a family of generalized d'Alembertian operators in D -dimensional Minkowski spacetimes \mathbb{M}^D which are manifestly Lorentz-invariant, retarded, and non-local, the extent of the nonlocality being governed by a single parameter ρ . The prototypes of these operators arose in earlier work as averages of matrix operators meant to describe the propagation of a scalar field in a causal set. We generalize the original definitions to produce an infinite family of “Generalized Causet Box (GCB) operators” parametrized by certain coefficients $\{a, b_n\}$, and we derive the conditions on the latter needed for the usual d'Alembertian to be recovered in the infrared limit. The continuum average of a GCB operator is an integral operator in \mathbb{M}^D , and it is these continuum operators that we mainly study. To that end, we compute their action on plane waves, or equivalently their Fourier transforms $g(p)$ [p being the momentum-vector]. For timelike p , $g(p)$ has an imaginary part whose sign depends on whether p is past or future-directed. For small p , $g(p)$ is necessarily proportional to $p \cdot p$, but for large p it becomes constant, raising the possibility of a genuinely Lorentzian perturbative regulator for quantum field theory in \mathbb{M}^D . We also address the question of whether or not the evolution defined by the GCB operators is stable, finding evidence that the original 4D causal set d'Alembertian is unstable, while its 2D counterpart is stable.

Contents

1	Introduction	1
2	The Original 2D and 4D Causet d’Alembertians	3
2.1	2D	3
2.2	4D	7
3	The Generalized Causet Box (GCB) Operators	9
3.1	Spectrum	10
3.2	IR Behaviour	11
3.3	UV Behaviour and the Retarded Green’s Function	12
3.4	A Possible Regularization Scheme for Quantum Field Theory	15
3.5	Stability	15
4	Summary and Remarks	17
A	IR Behaviour of the GCB Operators: Details	19
A.1	Even Dimensions	19
A.2	Odd Dimensions	20
B	UV Behaviour of the GCB Operators: Details	21
B.1	Even Dimensions	21
B.2	Odd Dimensions	22
C	Derivation of Equation (2.5)	23
D	Damping the fluctuations	24

1 Introduction

Causal set theory postulates that the fundamental structure of spacetime is that of a locally finite partially ordered set [1].¹ Its marriage of discreteness with causal order implies that physics cannot remain local at all scales. To appreciate why this should be, let us consider how one might define a notion of “closeness” in a causal set, confining ourselves to causal sets C which are obtained by randomly selecting points from a Lorentzian manifold M

¹ Characterized mathematically, this is a set C endowed with a binary relation \prec such that for all $x, y, z \in C$ the following axioms are satisfied: (1) transitivity: $x \prec y \ \& \ y \prec z \Rightarrow x \prec z$; (2) irreflexivity: $x \not\prec x$; (3): local finiteness: $|\{y \in C | x \prec y \prec z\}| < \infty$. Thus a causal set (causet) is in a certain sense both Lorentzian [in virtue of (1) and (2)] and discrete [in virtue of (3)].

and endowing the selected points with the causal relations inherited from the manifold.² Given such a causet, any intrinsically defined notion of closeness between two elements of C will reflect their Lorentzian distance in the embedding spacetime. But a small Lorentzian distance between two points of M does *not* mean that they are confined to a small neighbourhood within M . Rather, the second point can be “arbitrarily distant” from the first, as long as it is located near to the lightcone of the latter. Thus, an element of C will inevitably possess *very many* “nearest neighbours”, no matter how that notion is formalized. In this manner, the concept of locality provided by the topology of a continuous spacetime manifold is lost.

This nonlocality manifests itself concretely when one seeks to describe the wave propagation of a scalar field on a causal set by defining a discrete counterpart of the d’Alembertian operator, \square . For the aforementioned reasons, it seems impossible to proceed in analogy with what one does when, for example, one discretizes the Laplacian operator in a Riemannian spacetime. Nevertheless, a non-local operator was suggested in [2] which on average reproduces \square in the appropriate continuum limit for $1 + 1$ dimensional Minkowski space \mathbb{M}^2 (i.e. for causets derived by sprinkling \mathbb{M}^2). The expression introduced in [2] was generalized to $D = 4$ dimensions in [3] and recently to arbitrary D in [4].

We shall denote a discrete causal set d’Alembertian designed for \mathbb{M}^D by $B_\rho^{(D)}$, where ρ (dimensionally an inverse spacetime volume) is a volume-scale that controls the extent of the non-locality. In the case of causal sets which are well-approximated by D -dimensional Minkowski space \mathbb{M}^D , averaging $B_\rho^{(D)}$ over all such causets (i.e. averaging over all sprinklings of \mathbb{M}^D in the sense of footnote 2) leads to a *non-local* and retarded continuum operator $\square_\rho^{(D)}$ defined in \mathbb{M}^D . We shall refer to this operator as the *continuum causal set d’Alembertian*. Its crucial property is that it reproduces the usual d’Alembertian in the limit of zero non-locality scale: $\square_\rho^{(D)}\phi \rightarrow \square\phi$ as $\rho \rightarrow \infty$ for test-functions ϕ of compact support.

Although the causet operator $B_\rho^{(D)}$ is necessarily nonlocal, one might expect that the range of its nonlocality could be confined to the discreteness scale itself. In other words, one might expect that $\rho \sim \ell^{-4}$, ℓ being the — presumably Planckian — discreteness length. However, one can also cite reasons why one might need to have $\rho \ll \ell^{-4}$, leading to a more long-range nonlocality.³ Although these reasons are not conclusive, let us accept them

² This process is known as *Poisson sprinkling*: Given a spacetime M , let the discrete subset of points, C , be one particular realization of a Poisson process in M , and let the elements of C retain the causal relations they have when regarded as points of M . In order that the resulting precedence relation on C approximately encode the metric of M , one must exclude spacetimes with closed causal curves, for example by requiring M to be globally hyperbolic.

³ The issue here concerns the behavior of $B_\rho^{(D)}$ for one particular sprinkling versus its behavior after averaging over all sprinklings. The latter converges to \square as $\rho \rightarrow \infty$ but the former incurs fluctuations which grow larger as $\rho \rightarrow \infty$ and which therefore will be sizable if ρ is the sprinkling density, ℓ^{-4} . Which behavior is relevant physically? In full quantum gravity some sort of sum over different causets will be involved, including in particular a sum over sprinklings. Such a sum differs from a simple average and might or might not damp out the fluctuations, or they might cancel in other ways. But if neither of these things happens, the only way out [2] would be to choose ρ small enough that the necessary averaging will occur within each individual causet.

provisionally. A natural question then arises: might such a “mesoscopic” nonlocality show up at energy-scales accessible by current experiments?

Ideally, one would address this question in the fully discrete setting, but it seems much easier to begin with the continuum version of the same question by asking what changes when the local operator \square is replaced by the nonlocal operator $\square_\rho^{(D)}$. In this paper, we make a start on answering this question by analysing the “spectral properties” (Fourier transform) of a family of continuum operators $\square_\rho^{(D)}$. In Section 2, we discuss the continuum operators corresponding to the original 2D [2] and 4D [3] causet d’Alembertians, and in Section 3 we generalize the discussion to an infinite family of operators parametrized by a set of coefficients, $\{a, b_n\}$, for which we derive explicit equations that ensure the usual flat space d’Alembertian is recovered in the infrared limit. Based on the UV behaviour of these operators (which we determine for all dimensions and coefficients $\{a, b_n\}$), we propose a genuinely Lorentzian perturbative regulator for quantum field theory (QFT). Finally, we address the question of whether or not the evolution defined by the (classical) equation $\square_\rho^{(D)}\phi = 0$ is stable. We devise a numerical method to test for stability and present strong evidence that the original 4D causal set d’Alembertian is unstable in this sense, while its 2D counterpart is stable.

Throughout the paper we use the metric signature $(- + + \dots)$ and set $\hbar = c = 1$.

2 The Original 2D and 4D Causet d’Alembertians

In this Section we discuss the original continuum causet d’Alembertians for dimensions two [2] and four [3]. Let us start by establishing some terminology. Given any two elements x, y of a causal set C , we define the *order interval* $\text{Int}(x, y)$ between them as the set of all elements common to the (exclusive) future of x and the (exclusive) past of y : $\text{Int}(x, y) = \{z \in C \mid x \prec z \prec y\}$. Notice that in our convention, $\text{Int}(x, y)$ does not include x or y . An element $y \prec x$ is then considered a past n th neighbour of x if $\text{Int}(y, x)$ contains n elements. For instance, y is a 0th neighbour of x if $\text{Int}(y, x)$ is empty, a first neighbour if $\text{Int}(y, x)$ contains one element, and so on (see Figure 1 for an example). We denote the set of all past n th neighbours of x by $I_n(x)$.

Throughout the paper, we will only consider causal sets which are obtained by Poisson sprinklings of Minkowski space at density ρ .

2.1 2D

The original causet d’Alembertian for dimension 2, which we denote by $B_\rho^{(2)}$, acts on a scalar field $\Phi(x)$ on the causal set in the following way [2]:

$$\rho^{-1}(B_\rho^{(2)}\Phi)(x) = a^{(2)}\Phi(x) + \sum_{n=0}^2 b_n^{(2)} \sum_{y \in I_n(x)} \Phi(y), \quad (2.1)$$

where

$$a^{(2)} = -2, \quad b_0^{(2)} = 4, \quad b_1^{(2)} = -8, \quad b_2^{(2)} = 4. \quad (2.2)$$

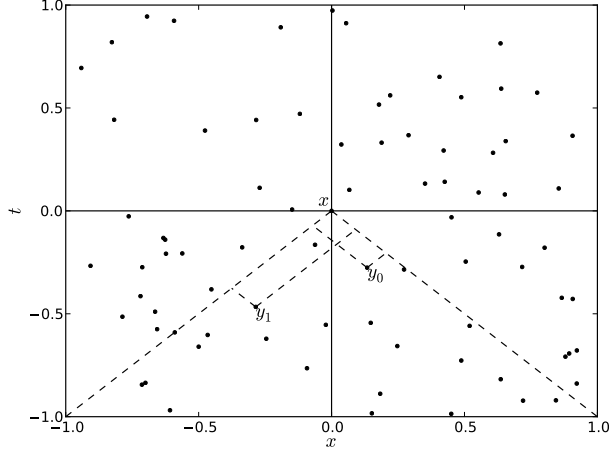


Figure 1: A Poisson sprinkling of $1 + 1$ Minkowski space at density $\rho = 80$. Here y_0 is a 0th neighbour of x because there are no elements which are both to the future of y_0 and the past of x . Similarly, y_1 is a first neighbour of x . The contributions of the points y_0 and y_1 to $\rho^{-1}(B_\rho^{(2)}\Phi)(x)$ are $b_0^{(2)}\Phi(y_0)$ and $b_1^{(2)}\Phi(y_1)$, respectively. The continuum limit, or rather average, of $(B_\rho^{(2)}\Phi)(x)$ can be understood as follows: fix the point x , keep sprinkling at density ρ and compute $(B_\rho^{(2)}\Phi)(x)$ for every sprinkling. The average of all these values is equal to $(\Box_\rho^{(2)}\Phi)(x)$.

Figure 1 illustrates how $B_\rho^{(2)}$ is defined, given a Poisson sprinkling of 2D Minkowski space \mathbb{M}^2 . The continuum operator $\Box_\rho^{(2)}$ is obtained by averaging $B_\rho^{(2)}$ over all such Poisson sprinklings at density ρ :

$$\rho^{-1}(\Box_\rho^{(2)}\Phi)(x) = a^{(2)}\Phi(x) + \rho \sum_{n=0}^2 \frac{b_n^{(2)}}{n!} \int_{J^-(x)} e^{-\rho V(x-y)} [\rho V(x-y)]^n \Phi(y) d^2y. \quad (2.3)$$

Here $J^-(x)$ denotes the causal past of x , and $V(x-y)$ is the spacetime volume enclosed by the past lightcone of x and the future lightcone of y . Note that $\Box_\rho^{(2)}$ is a *retarded* operator, in the sense that (2.3) uses information only from the causal past of x .

The operator $\Box_\rho^{(2)}$ can be studied by analysing its action on plane waves. Due to translation symmetry of Minkowski space,⁴ any plane wave $e^{ip \cdot x}$ is an eigenfunction of $\Box_\rho^{(2)}$ (provided that the integrals in (2.3) converge, so that the left hand side is well defined):

$$\Box_\rho^{(2)} e^{ip \cdot x} = g_\rho^{(2)}(p) e^{ip \cdot x}, \quad (2.4)$$

where $p \cdot x \equiv \eta_{\mu\nu} p^\mu x^\nu$ and $\eta_{\mu\nu} = \text{diag}(-1, 1)$. Interestingly enough, $g_\rho^{(2)}(p)$ in this case can be expressed in closed form:⁵

$$\rho^{-1} g_\rho^{(2)}(p) = -Z e^{Z/2} E_2(Z/2), \quad (2.5)$$

⁴ This is why the volume V in (2.3) is a function only of the difference, $x - y$.

⁵ This formula is derived in Appendix C, using the general formalism developed in Section 3.

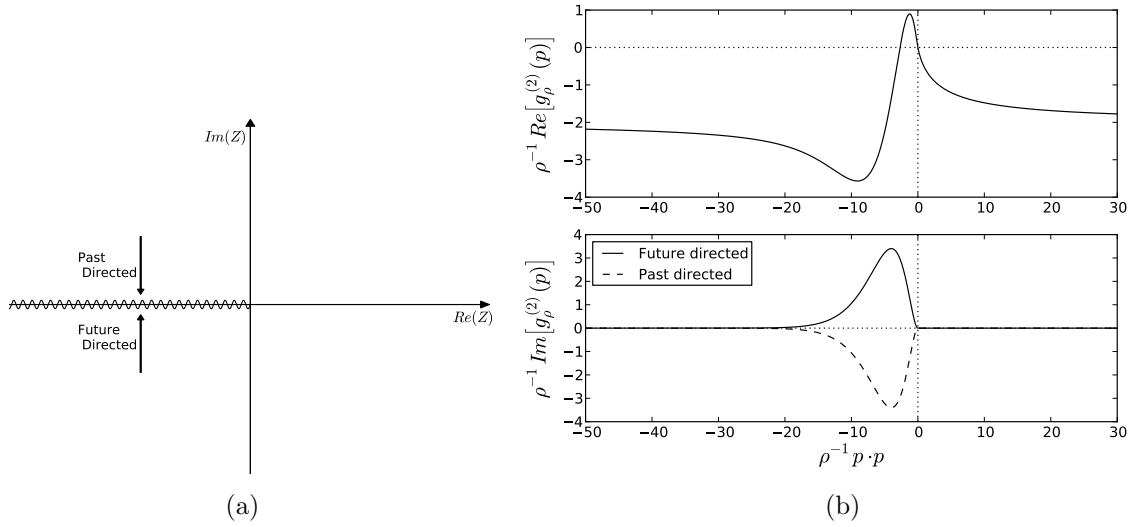


Figure 2: (a) The principal branch of $\rho^{-1}g_\rho^{(2)}(p)$, which (for real p) depends only on $Z = \rho^{-1}p \cdot p$, and on $\text{sgn}(p^0)$ when p is timelike. (b) The spectrum $g_\rho^{(2)}(p)$ of the original 2D continuum causet d'Alembertian for real momenta p . For spacelike momenta ($p \cdot p > 0$), $g^{(2)}(p)$ is real. For timelike momenta, it is complex with an imaginary part whose sign is opposite for past-directed and future-directed momenta.

where $E_2(z)$ is a generalized exponential integral function (see e.g. 8.19 of [5]) and

$$Z \equiv \rho^{-1}p \cdot p. \quad (2.6)$$

Here, as illustrated in Figure 2, $E_2(z)$ assumes its principal value, with a branch cut along the negative real axis. For real and spacelike momenta ($Z > 0$), $g^{(2)}$ is real. For real and timelike momenta ($Z < 0$), its value above/below the branch cut corresponds to past/future-directed momentum-vectors. There, $g_\rho^{(2)}$ is complex and changes to its complex conjugate across the cut. That the spectrum is different for past and future-directed momenta should come as no surprise, given that $\square_\rho^{(2)}$ is retarded by definition. We will see in Section 3 that these features persist in all dimensions and for a much broader class of causet d'Alembertians.

The infrared (IR) and ultraviolet (UV) behaviours of $g_\rho^{(2)}(p)$ are easily deduced from the asymptotic forms of $E_2(Z)$ (see e.g. 8.11.2, 8.19.1, and 8.19.8 of [5]):

$$\rho^{-1}g_\rho^{(2)}(p) \xrightarrow{Z \rightarrow 0} -Z + \dots \quad (2.7)$$

$$\rho^{-1}g_\rho^{(2)}(p) \xrightarrow{Z \rightarrow \infty} -2 + \frac{8}{Z} + \dots \quad (2.8)$$

The first of these two equations shows that the usual d'Alembertian \square is indeed reproduced in the limit of zero non-locality. The second equation, on the other hand, reveals a UV behaviour quite unlike that of the usual d'Alembertian; in Section 3.2 it will lead us to propose a new regularization scheme for quantum field theory.

An important question is whether the evolution defined by $\square_\rho^{(2)}\Phi = 0$ is stable or not. To a large extent this is answered by the fact that the only zero of $g_\rho^{(2)}(p)$ occurs at $Z = \rho^{-1}p \cdot p = 0$. To demonstrate this, we note that $g_\rho^{(2)}(p)$ has the following representation (see e.g. 8.19.1 and 8.6.4 of [5]):

$$\rho^{-1}g_\rho^{(2)}(p) = -Zf(Z), \quad f(Z) \equiv \int_0^\infty \frac{te^{-t}}{t + Z/2} dt. \quad (2.9)$$

It therefore suffices to prove that $f(Z)$ has no zeros when $Z \neq 0$. But the imaginary part of $f(Z)$ is

$$\text{Im}(f(Z)) = -\frac{\text{Im}(Z)}{2} \int_0^\infty \frac{te^{-t}}{\left[t + \frac{\text{Re}(Z)}{2}\right]^2 + \left[\frac{\text{Im}(Z)}{2}\right]^2} dt. \quad (2.10)$$

Because the integral that multiplies $-\text{Im}(Z)/2$ in (2.10) is strictly positive, $Zf(Z)$ could vanish only for real Z . Obviously, it does vanish for $Z = 0$, but elsewhere on the real axis, it remains nonzero, as illustrated in Figure 2b.

What we have just proven is that a plane wave solves the equation $\square_\rho^{(2)}\Phi = 0$ iff it solves the equation $\square\Phi = 0$. To the extent that the general solutions of these two wave equations can be composed of plane waves, they therefore share the same space of solutions. This, of course, is an important result in itself. But it also, a fortiori, answers the stability question in the affirmative, since we know that the evolution corresponding to \square is stable.

If there remains any doubt about stability or about the fact that both $\square\Phi = 0$ and $\square_\rho^{(2)}\Phi = 0$ yield the same evolution, it springs from a possible uncertainty about boundary conditions. In the usual situation (that of the ordinary d'Alembertian \square), one understands how to relate a general solution to its initial data on an arbitrary Cauchy surface, and when Φ falls off suitably at infinity, its total energy is defined and conserved. From energy conservation, stability also follows — relative to the given choice of boundary conditions. On the other hand in the case of $\square_\rho^{(2)}$, a connection between solutions and Cauchy data remains to be found, as does a better understanding of appropriate falloff conditions. But absent some such boundary condition there is nothing to exclude complex momenta p that lead to exponential growth in time, e.g. an imaginary multiple of a real lightlike vector.

For these reasons, we would like to discuss stability from a slightly different angle, which also will be helpful when we come to deal with the 4D case. Quite generally, instabilities tend to be associated with exponentially growing “modes” (in this case plane waves). Let us then *assume* that we can take this as our criterion of (in)stability. And to exclude the kind of “fake instability” mentioned above, let us also require any putative unstable mode, $\Phi(x) = e^{ip \cdot x}$, to be bounded at spatial infinity in at least one Lorentz frame. (Unfortunately we cannot say “in all Lorentz frames”, since for a plane wave, exponential growth in time induces exponential growth in space via a Lorentz boost.) We might hope that the condition just formulated is equivalent to the following more natural one: consider only solutions of $\square_\rho^{(2)}\Phi(x) = 0$ which have compact support on every Cauchy hypersurface (compact spatial support in every frame.)

Be that as it may, if this criterion is accepted, then we can establish stability very simply in the present case, because an unstable mode, $\Phi(x) = e^{ip \cdot x}$, is then precisely

one such that p possesses a future-directed timelike imaginary part: $p = p_R + ip_I$ with $p_I \cdot p_I < 0$ and $p_I^0 > 0$. This, however, is impossible for $Z = 0$, as one sees from the equation $0 = p \cdot p = p_R \cdot p_R - p_I \cdot p_I + 2ip_R \cdot p_I$, whose right-hand side has a strictly positive real part when p_I is timelike. For logical completeness, we should also observe that (2.5) is valid for all complex p whose imaginary parts are timelike and future-directed. (For more general complex momenta, the integral defining $\square_\rho^{(2)}\Phi$ might not converge, a circumstance that, depending once again on the choice of falloff conditions, might or might not impinge on the claimed identity between our solutions and those of the ordinary wave equation.)

2.2 4D

The causet d'Alembertian for dimension 4, has the same general form as that for \mathbb{M}^2 , but with different coefficients [3] :

$$\rho^{-\frac{1}{2}}(B_\rho^{(4)}\Phi)(x) = a^{(4)}\Phi(x) + \sum_{n=0}^3 b_n^{(4)} \sum_{y \in I_n(x)} \Phi(y), \quad (2.11)$$

where

$$a^{(4)} = -\frac{4}{\sqrt{6}}, \quad b_0^{(4)} = \frac{4}{\sqrt{6}}, \quad b_1^{(4)} = -\frac{36}{\sqrt{6}}, \quad b_2^{(4)} = \frac{64}{\sqrt{6}}, \quad b_3^{(4)} = -\frac{32}{\sqrt{6}}. \quad (2.12)$$

The continuum average $\square_\rho^{(4)}$ then also takes a similar form:

$$\rho^{-\frac{1}{2}}(\square_\rho^{(4)}\Phi)(x) = a^{(4)}\Phi(x) + \rho \sum_{n=0}^3 \frac{b_n^{(4)}}{n!} \int_{J^-(x)} e^{-\rho V(x-y)} [\rho V(x-y)]^n \Phi(y) d^4y. \quad (2.13)$$

We will show in Section 3.1 that the “spectrum” of $\square_\rho^{(4)}$, as defined by $\square_\rho^{(4)}e^{ip \cdot x} = g_\rho^{(4)}(p)e^{ip \cdot x}$, is given by

$$\rho^{-1/2}g_\rho^{(4)}(p) = a^{(4)} + 4\pi Z^{-1/2} \sum_{n=0}^3 \frac{b_n^{(4)}}{n!} C_4^n \int_0^\infty s^{4n+2} e^{-C_4 s^4} K_1(Z^{1/2}s) ds, \quad (2.14)$$

where K_1 is a modified Bessel function of the second kind and

$$Z \equiv \rho^{-1/2}p \cdot p, \quad C_4 = \frac{\pi}{24}. \quad (2.15)$$

All functions in (2.14) assume their principal values with branch cuts along the negative real axis. Many properties of the 2D function $g_\rho^{(2)}(p)$ carry over to $g_\rho^{(4)}(p)$. For timelike p , the value of $g_\rho^{(4)}(p)$ above/below the branch cut corresponds to past/future-directed momenta, and it changes to its complex conjugate across the cut. Also, $g_\rho^{(4)}$ is real for spacelike momenta. Figure 3b shows the behaviour of $g_\rho^{(4)}(p)$ for real momenta.

The IR and UV behaviours of $g_\rho^{(4)}(p)$, which are derived in Sections 3.2 and 3.3, are given by

$$\rho^{-1/2}g_\rho^{(4)}(p) \xrightarrow{Z \rightarrow 0} -Z + \dots \quad (2.16)$$

$$\rho^{-1/2}g_\rho^{(4)}(p) \xrightarrow{Z \rightarrow \infty} -\frac{4}{\sqrt{6}} + \frac{32\pi}{\sqrt{6}Z^2} + \dots \quad (2.17)$$

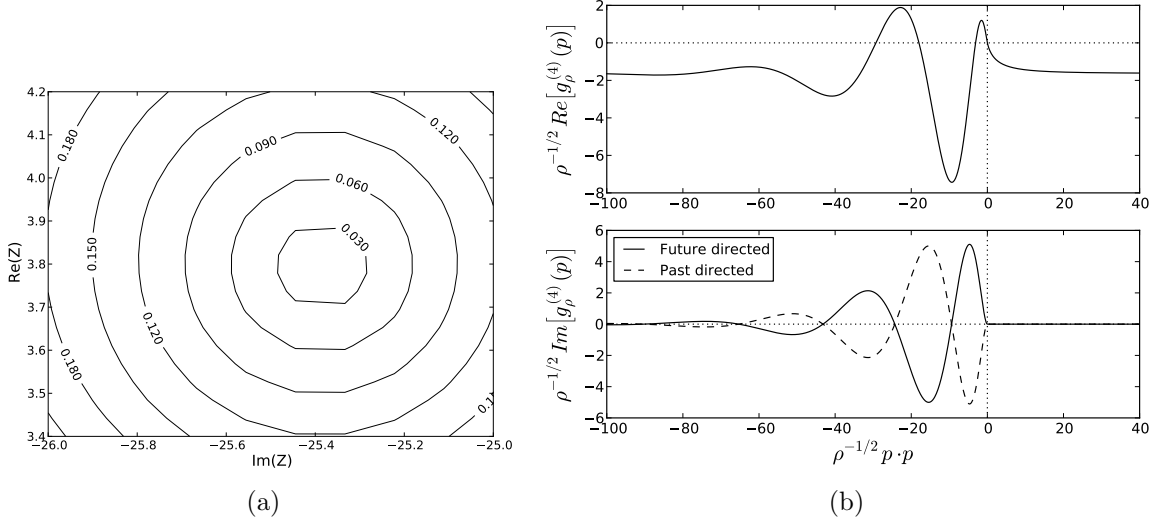


Figure 3: (a) An unstable zero of $g_\rho^{(4)}(p)$. Contours of constant $|\rho^{-1/2}g_\rho^{(4)}|$ are plotted as a function of the real and imaginary parts of $Z = \rho^{-1/2}p \cdot p$. (b) Spectrum $g_\rho^{(4)}(p)$ of the original 4D causet d'Alembertian for real momenta p . For spacelike momenta ($p \cdot p > 0$), $g^{(4)}(p)$ is real. For timelike momenta, it contains also an imaginary part whose sign is opposite for past-directed and future-directed momentum-vectors.

Again, the IR behaviour confirms that the usual d'Alembertian is reproduced in the limit of zero non-locality. The UV limit has the form of a constant plus a term proportional to p^{-4} . The inverse of $g_\rho^{(4)}(p)$, which defines the retarded Green's function in Fourier space, takes exactly the same form in the UV:

$$\frac{\rho^{1/2}}{g_\rho^{(4)}(p)} \xrightarrow{Z \rightarrow \infty} -\frac{\sqrt{6}}{4} - \frac{2\pi\sqrt{6}}{Z^2} + \dots \quad (2.18)$$

In any QFT based on $\square_\rho^{(4)}$, the propagator associated with internal lines in Feynman diagrams would presumably have the same UV behaviour. Subtracting the constant term from the propagator (which corresponds to subtracting a δ -function in real space) would then render all loops finite. This procedure could be the basis of a genuinely Lorentzian regularization and renormalization scheme for QFT. We will discuss these things more generally in Sections 3.3 and 3.4.

We have only been able to address the question of stability by numerical means in this case, and we refer the reader to Section 3.5. It turns out that $g_\rho^{(4)}(p)$ does in fact have unstable modes in the sense that there exist complex momentum-vectors p which satisfy $g_\rho^{(4)}(p) = 0$, and whose imaginary parts are timelike and future-directed. Such a mode corresponds to a complex zero of $g_\rho^{(4)}$ in the complex Z -plane, and Figure 3a shows one such zero (the other one being its complex conjugate).

3 The Generalized Causet Box (GCB) Operators

The key property of the causet d'Alembertians introduced in the previous Section is that they reproduce \square in the continuum-averaged (averaged over all sprinklings) and local ($\rho \rightarrow \infty$) limit. In this Section, we explore a larger family of operators $B_\rho^{(D)}$ which share the same property. We place the following conditions on $B_\rho^{(D)}$:

1. **Linearity:** when $B_\rho^{(D)}$ acts on a scalar field Φ , the result at an element x of the causet should be a linear combination of the values of Φ at other elements y (possibly including x itself). This is a natural requirement because \square itself is linear.
2. **Retardedness:** $(B_\rho^{(D)}\Phi)(x)$ should depend only on $\Phi(y)$, with y in the causal past of x . This requirement allows for a consistent evolution of a partial solution specified on any “downward closed” subset of the causet.
3. **Label invariance:** $B_\rho^{(D)}$ should be invariant under relabellings of causal set elements. This is the discrete analogue of general covariance.
4. **Neighbourly democracy:** all n th neighbours of x should contribute to $(B_\rho^{(D)}\Phi)(x)$ with the same coupling.

Considering all these requirements, $(B^{(D)}\Phi)(x)$ can be expressed in the following general form

$$\rho^{-\frac{2}{D}}(B_\rho^{(D)}\Phi)(x) = a\Phi(x) + \sum_{n=0}^{L_{max}} b_n \sum_{y \in I_n(x)} \Phi(y), \quad (3.1)$$

where $\{a, b_n\}$ are dimensionless coefficients and $I_n(x)$ is the set of all n th neighbours to the past of x (see beginning of Section 2). This is a straightforward generalization of (2.1) and (2.11), where we have now allowed ourselves up to L_{max} neighbours. We will soon see that recovering \square requires keeping a *minimum* number of layers: e.g. $L_{max} \geq 2$ in 2D and $L_{max} \geq 3$ in 4D. The original 2D and 4D proposals are then the minimal cases in this sense.

The continuum-average $\square_\rho^{(D)}$ of $B_\rho^{(D)}$ acts on a scalar field $\Phi(x)$ in the following way:

$$\rho^{-2/D}(\square_\rho^{(D)}\Phi)(x) = a\Phi(x) + \rho \sum_{n=0}^{L_{max}} \frac{b_n}{n!} \int_{J^-(x)} e^{-\rho V(x,y)} [\rho V(x,y)]^n \Phi(y) d^D y. \quad (3.2)$$

Here as before, $J^-(x)$ denotes the causal past of x , while $V(x,y)$ is the spacetime volume enclosed by the past light cone of x and the future light cone of y .

The occurrence of the factor $e^{-\rho V}$ in (3.2) shows that the parameter ρ (which dimensionally is an energy-density) functions as a kind of “nonlocality scale” controlling the distance over which the operator $\square_\rho^{(D)}$ acts. As our definitions stand so far, this nonlocality-scale directly reflects the fundamental discreteness-scale, because (3.2) was derived under the assumption that ρ was the sprinkling-density in \mathbb{M}^D . However it turns out that one can decouple the two scales by tweaking the definition (3.1) in such a way as to produce a more general causet operator whose sprinkling-average reproduces the same continuum operator

(3.2), even when ρ is smaller than the sprinkling density. With this operator, the nonlocality can extend over a much greater distance than that of the fundamental discreteness-scale. Although modifying $B_\rho^{(D)}$ in this way has the disadvantage of introducing a second, independent length scale, it allows one to overcome a potential difficulty pointed out in [2], namely that (3.1) with fixed coefficients leads to fluctuations in $(B_\rho^{(D)}\Phi)(x)$ which grow with ρ , rather than diminishing. We have provided the definition of this “tweaked” operator and the derivation of its continuum average in Appendix D; but henceforth, we will concern ourselves exclusively with the continuum operator $\square_\rho^{(D)}$, without worrying about its relationship with any underlying discreteness. Correspondingly, ρ will henceforth denote a non-locality-scale with no necessary relation to any discreteness scale.

3.1 Spectrum

That any plane wave $e^{ip \cdot x}$ is an eigenfunction of $\square_\rho^{(D)}$ in \mathbb{M}^D follows from translational symmetry: $V(x, y) = V(x - y)$. It can be shown in fact that

$$\square_\rho^{(D)} e^{ip \cdot x} = g_\rho^{(D)}(p) e^{ip \cdot x}, \quad (3.3)$$

$$\rho^{-2/D} g_\rho^{(D)}(p) = a + \sum_{n=0}^{L_{max}} \frac{(-1)^n \rho^{n+1}}{n!} b_n \frac{\partial^n}{\partial \rho^n} \chi(p, \rho), \quad (3.4)$$

$$\chi(p, \rho) = \int_{J^+(0)} e^{-\rho V(y)} e^{-ip \cdot y} d^D y, \quad (3.5)$$

where $V(y) = V(O, y)$ is the spacetime volume enclosed by the past light cone of y and the future light cone of the origin:

$$V(y) = C_D |y \cdot y|^{D/2}, \quad C_D = \frac{\left(\frac{\pi}{4}\right)^{\frac{D-1}{2}}}{D\Gamma(\frac{D+1}{2})}. \quad (3.6)$$

Evaluating $\chi(p, \rho)$ amounts to computing the Laplace transform of a retarded, Lorentz-invariant function, which has been done in [6]. It follows from their result that

$$\chi(p, \rho) = 2(2\pi)^{D/2-1} (p \cdot p)^{\frac{2-D}{4}} \int_0^\infty s^{D/2} e^{-\rho C_D s^D} K_{\frac{D}{2}-1}(\sqrt{p \cdot p} s) ds, \quad (3.7)$$

where K_ν is the modified Bessel function of the second kind. All functions in (3.7) assume their principal values, with a branch cut along the negative real axis. This result is valid for all p whose imaginary part is timelike and future-directed, i.e. $p_I \cdot p_I < 0$ and $p_I^0 > 0$, where $p = p_R + ip_I$ and the Lorentzian norm is given by $p \cdot p = p_R \cdot p_R - p_I \cdot p_I + 2ip_R \cdot p_I$. For momenta satisfying these conditions, the integral that defines $\chi(p, \rho)$, and consequently $\square_\rho^{(D)} e^{ip \cdot x}$, is absolutely convergent. Plugging (3.7) into (3.4) we find

$$\rho^{-2/D} g_\rho^{(D)}(p) = a + 2(2\pi)^{D/2-1} Z^{\frac{2-D}{4}} \sum_{n=0}^{L_{max}} \frac{b_n}{n!} C_D^n \int_0^\infty s^{D(n+1/2)} e^{-C_D s^D} K_{\frac{D}{2}-1}(Z^{1/2} s) ds,$$

(3.8)

where Z is a dimensionless quantity defined by

$$Z \equiv \rho^{-\frac{2}{D}} p \cdot p. \quad (3.9)$$

For real $p = p_R$, $g_\rho^{(D)}(p)$ can be defined by first adding a small future-pointing and timelike imaginary part p_I^ϵ to p_R , and then taking the limit as p_I^ϵ shrinks:

$$g_\rho^{(D)}(p_R) := \lim_{\epsilon \rightarrow 0^+} g_\rho^{(D)}(p_R + i p_I^\epsilon), \quad p_I^\epsilon \cdot p_I^\epsilon = -\epsilon^2. \quad (3.10)$$

When p_R is timelike, this amounts to changing $Z = \rho^{-\frac{2}{D}} p_R \cdot p_R$ on the right hand side of (3.8) to $Z + i\epsilon$ for past-directed, and $Z - i\epsilon$ for future-directed p_R . This is illustrated in Figure 2a. Because of the appearance of $Z^{1/2}$ in (3.8) and the fact that $K_\nu(\bar{z}) = \overline{K_\nu(z)}$, it follows for timelike p that

$$g_\rho^{(D)}(-p) = \overline{g_\rho^{(D)}(p)}. \quad (3.11)$$

Therefore, $g_\rho^{(D)}(p)$ differs for past- and future-directed timelike p . This is to be expected, since requiring $\square_\rho^{(D)}$ to be retarded builds in a direction of time. For spacelike momenta ($Z > 0$), $g_\rho^{(D)}(p)$ is real, as follows from the fact that $K_\nu(z)$ is real when ν is real and $\text{ph}(z) = 0$ [5].

3.2 IR Behaviour

We want to choose the coefficients a and b_n so that the usual d'Alembertian operator is recovered in the limit of zero non-locality:

$$\lim_{\rho \rightarrow \infty} \square_\rho^{(D)} \phi = \square \phi. \quad (3.12)$$

This requirement is equivalent to demanding

$$g_\rho^{(D)}(p) \xrightarrow{Z \rightarrow 0} -p \cdot p. \quad (3.13)$$

In Appendix A, we derive equations for a and b_n which guarantee this behaviour for an arbitrary spacetime dimension D . We expand $Z^{\frac{2-D}{4}} K_{\frac{D}{2}-1}(Z^{1/2}s)$ on the right hand side of (3.8) about $Z = 0$, and arrange a, b_n so that the terms which grow faster than Z vanish, while the coefficient of the term proportional to Z is -1 . We state the main results here and refer the reader to Appendix A for the details.

In **even dimensions**, letting $D = 2N + 2$ with $N = 0, 1, 2, \dots$, the equations that need to be satisfied are

$$\sum_{n=0}^{L_{max}} \frac{b_n}{n!} \Gamma\left(n + \frac{k+1}{N+1}\right) = 0, \quad k = 0, 1, \dots, N+1 \quad (3.14a)$$

$$a + \frac{2(-1)^{N+1} \pi^N}{N! D^2 C_D} \sum_{n=0}^{L_{max}} b_n \psi(n+1) = 0, \quad (3.14b)$$

$$\sum_{n=0}^{L_{max}} \frac{b_n}{n!} \Gamma\left(n + \frac{N+2}{N+1}\right) \psi\left(n + \frac{N+2}{N+1}\right) = \frac{2(-1)^N (N+1)!}{\pi^N} D^2 C_D^{\frac{N+2}{N+1}}, \quad (3.14c)$$

where $\psi(n)$ is the digamma function. Equations (3.14a) and (3.14c) determine b_n , after which (3.14b) fixes a . The minimum number of terms required to solve these equations is determined by $L_{max} \geq N + 2$. In 2D and 4D in particular, keeping this minimum number of terms leads to the solutions (2.2) and (2.12), respectively.

In **odd dimensions**, letting $D = 2N + 1$ with $N = 0, 1, 2, \dots$, the equation are

$$\sum_{n=0}^{L_{max}} \frac{b_n}{n!} \Gamma(n + \frac{2k+2}{2N+1}) = 0, \quad k = 0, 1, \dots, N \quad (3.15a)$$

$$a + \frac{(-1)^N \pi^{N+\frac{1}{2}}}{DC_D \Gamma(N + \frac{1}{2})} \sum_{n=0}^{L_{max}} b_n = 0, \quad (3.15b)$$

$$\sum_{n=0}^{L_{max}} \frac{b_n}{n!} \Gamma(n + \frac{2N+3}{2N+1}) = \frac{4(-1)^{N-1} \Gamma(N + \frac{3}{2})}{\pi^{N+\frac{1}{2}}} DC_D^{\frac{2N+3}{2N+1}}. \quad (3.15c)$$

Similarly to the even case, Equations (3.15a) and (3.15c) determine b_n , after which (3.15b) fixes a . The minimum number of terms is determined by $L_{max} \geq N + 1$.

3.3 UV Behaviour and the Retarded Green's Function

The UV behaviour of $g_\rho^{(D)}(p)$, as derived in Appendix B, is

$$\rho^{-2/D} g_\rho^{(D)}(p) \xrightarrow{Z \rightarrow \infty} a + 2^{D-1} \pi^{\frac{D}{2}-1} \Gamma(D/2) b_0 Z^{-\frac{D}{2}} + \dots \quad (3.16)$$

Thus, $g_\rho^{(D)}(p)$ behaves as a constant plus a term proportional to $(p \cdot p)^{-D/2}$. Let us explore the consequences of this fact for the retarded Green's function $G_R(x, y)$ associated with $\square_\rho^{(D)}$, which satisfies the usual equation

$$\square_\rho^{(D)} G_R(x, y) = \delta^{(D)}(x - y), \quad (3.17)$$

subject to the boundary condition $G_R(x, y) = 0 \ \forall \ x \not\prec y$.

Of course, translation invariance implies $G_R(x, y) = G_R(x - y)$. The Fourier transform $\tilde{G}_R(p)$ of $G_R(x - y)$ is given by the reciprocal of $g_\rho^{(D)}(p)$:

$$G_R(x - y) = \int \frac{d^D p}{(2\pi)^D} \tilde{G}_R(p) e^{ip \cdot (x-y)} = \int \frac{d^D p}{(2\pi)^D} \frac{1}{g_\rho^{(D)}(p)} e^{ip \cdot (x-y)}. \quad (3.18)$$

Figure 4a shows the path of integration in the complex p^0 plane. When $g_\rho^{(D)}(p)$ has no zero in complex plane apart from at $p \cdot p = 0$, this choice of contour ensures that G_R is indeed retarded. As we will argue in the next section, the presence of such zeros implies that evolution defined by $\square_\rho^{(D)}$ is unstable. Therefore, we shall ignore these cases for our current discussion.

The behaviour of $G_R(x - y)$ in the coincidence limit $x \rightarrow y$ is determined by the behaviour of $\tilde{G}_R(p)$ at large momenta:

$$\rho^{2/D} \tilde{G}_R(p) \xrightarrow{Z \rightarrow \infty} \frac{1}{a} - 2^{D-1} \pi^{\frac{D}{2}-1} \Gamma(D/2) \frac{b_0}{a^2} Z^{-\frac{D}{2}} + \dots \quad (3.19)$$

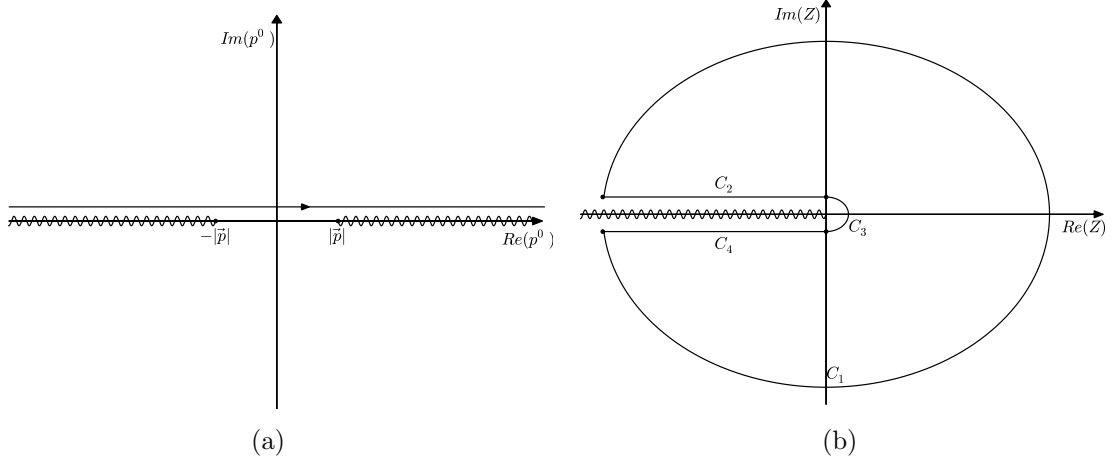


Figure 4: (a) The integration path in the complex p^0 plane which defines the retarded Green's function. (b) The contour of integration used for counting the unstable modes of $\square_\rho^{(D)}$. The direction of integration is taken to be counter-clockwise.

Here we have assumed $a \neq 0$. When $a = 0$, $\tilde{G}_R(p)$ scales as p^D for large momenta, a badly divergent UV behaviour. Therefore we will confine ourselves to cases where $a \neq 0$.

The constant term $\frac{1}{a}$ represents a δ -function in real space. The other terms in the series have the form $\int d^D p p^{-nD}$, $n = 1, 2, \dots$, and it can be shown that they are all finite. It then looks like subtracting $\frac{1}{a}\delta^{(D)}(x-y)$ from $\rho^{2/D}G_R(x-y)$ must result in a completely smooth function in the coincidence limit, and we will now show this is indeed the case.

Although $D = 4$ is the dimension of greatest interest, the proof which we shall present is valid in all even dimensions. Let us define

$$\rho^{2/D}G(x-y) \equiv \rho^{2/D}G_R(x-y) - \frac{1}{a}\delta^{(D)}(x-y). \quad (3.20)$$

Our task is then to show $G(x-y)$ is a smooth function at $x = y$. It follows from (3.18) that

$$\rho^{2/D}G(x-y) = \int \frac{d^D p}{(2\pi)^D} \left[\frac{1}{\rho^{-2/D}g_\rho^{(D)}(p)} - \frac{1}{a} \right] e^{ip \cdot (x-y)}. \quad (3.21)$$

Because $G_R(x-y)$ is retarded by definition,

$$\int \frac{d^D p}{(2\pi)^D} \frac{1}{g_\rho^{(D)}(p)} e^{ip \cdot (x-y)} = 0, \quad x \not\succ y. \quad (3.22)$$

From this it follows for all $x \succ y$ that

$$\int \frac{d^D p}{(2\pi)^D} \frac{1}{g_\rho^{(D)}(p)} e^{ip \cdot (x-y)} = \int \frac{d^D p}{(2\pi)^D} \frac{1}{g_\rho^{(D)}(p)} e^{-ip \cdot (x-y)} \stackrel{x \succ y}{=} 0, \quad (3.23)$$

where the first equality is obtained by changing $p \rightarrow -p$ and then using (3.11), and the second equality is a direct consequence of (3.22) with x and y interchanged. Returning to

(3.21), and subtracting zero in the form of (3.23), we obtain

$$G(x-y) \stackrel{x \succ y}{=} \int \frac{d^D p}{(2\pi)^D} \left[\frac{1}{g_\rho^{(D)}(p)} - \frac{1}{\overline{g_\rho^{(D)}(p)}} \right] e^{ip \cdot (x-y)} \quad (3.24)$$

$$= \int_{p^2 < 0} \frac{d^D p}{(2\pi)^D} \left[\frac{1}{g_\rho^{(D)}(p)} - \frac{1}{\overline{g_\rho^{(D)}(p)}} \right] e^{ip \cdot (x-y)}, \quad (3.25)$$

where the second equality is true because $g_\rho^{(D)}(p)$ is real for space-like momenta. (Note that the $\frac{1}{a}$ term contributes only when $x = y$.) In what follows, we let

$$\rho^{-2/D} g_\rho^{(D)}(p) \equiv \tilde{g}(Z), \quad (3.26)$$

as given in the right hand side of (3.8).

The integral in (3.25) can be divided into two integrals over $p^0 > 0$ and $p^0 < 0$. For a fixed sign of p^0 , $g_\rho^{(D)}(p)$ is only a function of $p \cdot p$, making (3.25) the Laplace transform of a Lorentz-invariant function. Similarly to how we derived (3.7), we use the result of [6] to compute $G(x-y)$:

$$\begin{aligned} \rho^{2/D} G(x-y) &\stackrel{x \succ y}{=} \frac{2}{\pi(2\pi)^{D/2}} \int_0^\infty d\xi \xi^{D/2} \\ &\times \text{Re} \left[\left(\sqrt{s_\epsilon^2} \right)^{1-\frac{D}{2}} K_{\frac{D}{2}-1}(\sqrt{s_\epsilon^2} \xi) \left(\frac{1}{\tilde{g}(-\xi^2 + i\epsilon)} - \frac{1}{\overline{\tilde{g}(-\xi^2 + i\epsilon)}} \right) \right], \end{aligned} \quad (3.27)$$

where $s_\epsilon^2 = -(t_x - t_y + i\epsilon)^2 + |\vec{r}_x - \vec{r}_y|^2$ and ϵ is a small positive number which should be taken to zero at the end of calculations. When $x-y$ is timelike and future-directed, we can let $\sqrt{s_\epsilon^2} = -i\tau_{xy}$ where $\tau_{xy} > 0$. Using properties of Bessel functions (see e.g. 10.27.9 of [5]), (3.27) can be simplified into the following form for even D:

$$\begin{aligned} \rho^{2/D} G(x-y) &\stackrel{x \succ y}{=} \frac{-i(-1)^{\frac{D}{2}} \tau_{xy}^{1-\frac{D}{2}}}{(2\pi)^{D/2}} \int_0^\infty d\xi \xi^{D/2} \left(\frac{1}{\tilde{g}(-\xi^2 + i\epsilon)} - \frac{1}{\overline{\tilde{g}(-\xi^2 + i\epsilon)}} \right) J_{\frac{D}{2}-1}(\tau_{xy}\xi) \\ &= \frac{2(-1)^{1+\frac{D}{2}} \tau_{xy}^{1-\frac{D}{2}}}{(2\pi)^{D/2}} \int_0^\infty d\xi \xi^{D/2} \frac{\text{Im} [\tilde{g}(-\xi^2 + i\epsilon)]}{|\tilde{g}(-\xi^2 + i\epsilon)|^2} J_{\frac{D}{2}-1}(\tau_{xy}\xi). \end{aligned} \quad (3.28)$$

Using $(x/2)^{1-D/2} J_{\frac{D}{2}-1}(x) \xrightarrow{x \rightarrow 0} \Gamma(D/2)^{-1}$ (see e.g. 10.2.2 of [5]) and the fact that $\text{Im} [\tilde{g}(-\xi^2 + i\epsilon)]$ is exponentially damped for large ξ (see Appendix B.1), it can be verified that

$$\lim_{x \rightarrow y} \rho^{2/D} G(x-y) = \frac{2^{2-\frac{D}{2}} (-1)^{1+\frac{D}{2}}}{(2\pi)^{\frac{D}{2}} \Gamma(\frac{D}{2})} \int_0^\infty d\xi \xi^{D-1} \frac{\text{Im} [\tilde{g}(-\xi^2 + i\epsilon)]}{|\tilde{g}(-\xi^2 + i\epsilon)|^2}. \quad (3.29)$$

Thus $G(x - y)$ approaches a constant in the coincidence limit.⁶ Strictly speaking, the discussion above only analyzes the behavior of $G(x - y)$ as τ_{xy} approaches 0, and consequently it does not exclude the presence of terms which blow up discontinuously on the light cone, such as $\delta(\tau_{xy}^2)$. However, a similar treatment for the case where $x - y \neq 0$ is null rather than timelike removes this loophole.

3.4 A Possible Regularization Scheme for Quantum Field Theory

As was shown in the previous Section, changing the usual d’Alembertian to the nonlocal operator $\square_\rho^{(D)}$ makes the coincidence limit more divergent, rather than smoothing it out as one might have initially expected. But it does so in an interesting way: all the divergences have now been absorbed into one δ -function at $x = y$. This feature has a natural application as a regularization tool for quantum field theory. In any QFT based on $\square_\rho^{(D)}$, one would expect the propagator associated with internal lines in Feynman diagrams to have the same UV behaviour as (3.19). Subtracting the constant term in (3.19) (which corresponds to subtracting a δ -function in real space) would then render all loops finite. This would be a genuinely Lorentzian regulator, with no need for Wick rotation. It would also be physically motivated, with the “UV completion” being understood as a theory on the causal set. It would be interesting to apply this technique to the renormalization of some well-understood scalar field theories.

3.5 Stability

Is the evolution defined by $\square_\rho^{(D)}$ stable? As we discussed in Section 2.1, instabilities are in general associated with “unstable modes”, and we agreed to use this as our criterion of instability for purposes of this paper. More specifically, we took such a mode to be a plane-wave $\Phi(x) = e^{ip \cdot x}$ satisfying the equation of motion $\square_\rho^{(D)} \Phi(x) = 0$, with the wave-vector p possessing a future-directed timelike imaginary part (i.e. $p = p_R + ip_I$ where $p_I \cdot p_I < 0$ and $p_I^0 > 0$).

The necessary and sufficient condition for avoiding unstable modes is then

$$\tilde{g}(Z) \neq 0, \quad \forall Z \neq 0, \quad (3.30)$$

where $\tilde{g}(Z)$ is defined in (3.26). Let us argue why this is the case. First observe that plane solutions of our wave-equation correspond exactly with zeros of $\tilde{g}(Z)$. If the above condition is verified, then the only such zero is at $Z = 0$, just as for the usual d’Alembertian. But we know (as is also easy to demonstrate ab initio) that there are no unstable modes in the usual case. Conversely, when the above condition is violated for some complex $Z \neq 0$, it is always possible to find a corresponding p with a timelike and future-directed

⁶One can understand intuitively why $G_R(x - y)$ is the sum of a δ -function with a bounded remainder by noticing that (up to an overall numerical factor) our nonlocal d’Alembertian operator has the form $1 - S$, where the ‘1’ corresponds to the first term in (2.3) or (3.2) and the remainder S is given by an integral-kernel which is both bounded and retarded. The inverse operator G_R would then be $G_R = (1 + S)^{-1} = 1 + SG_R = 1 + S + S^2 + S^3 \dots$, a series that should converge sufficiently near to $x = y$. Since the operator 1 is represented by a term of $\delta(x - y)$ in $G_R(x - y)$, one sees that $G_R(x - y)$ is the sum of a δ -function with a term involving only smooth bounded functions.

imaginary part which satisfies $p \cdot p = \rho^{\frac{2}{D}} Z$. To see this, we let $p = p_R + ip_I$ and take $p_R = \langle \pi_R^0, \vec{\pi}_R \rangle$ and $p_I = \langle \pi_I, \vec{0} \rangle$ with $\pi_I > 0$. This is always possible because p_I is timelike and future-directed. The equations that need to be satisfied are

$$p_R \cdot p_R - p_I \cdot p_I = \rho^{\frac{2}{D}} \text{Re}(Z), \quad 2p_R \cdot p_I = \rho^{\frac{2}{D}} \text{Im}(Z). \quad (3.31)$$

Substituting for p_I leads to

$$\pi_R^0 = \frac{\rho^{\frac{2}{D}} \text{Im}(Z)}{-2\pi_I}, \quad |\vec{\pi}_R|^2 = \rho^{\frac{2}{D}} \text{Re}(Z) + \frac{\rho^{\frac{4}{D}} \text{Im}(Z)^2}{4\pi_I^2} - \pi_I^2. \quad (3.32)$$

This system of equations always has a solution. In fact, there is a whole family of such unstable modes parametrized by π_I . Note however that the condition $|\vec{\pi}_R|^2 > 0$ puts an upper bound on the value of π_I , and therefore on the growth rate of such an instability.

We have thus reduced the question of whether or not $\square_\rho^{(D)}$ has unstable modes to the question of whether $\tilde{g}(Z)$ has zeros other than $Z = 0$ in the complex plane. We can answer this question by counting the zeros of $\tilde{g}(Z)$ with the aid of the “argument principle” of complex analysis:

$$\frac{1}{2\pi i} \oint_C \frac{\tilde{g}'(Z)}{\tilde{g}(Z)} dZ = N - P, \quad (3.33)$$

where N and P are the number of zeros and poles, respectively, inside of the closed contour C , which we choose as shown in Figure 4b. The number of poles inside C is zero because all terms appearing in $\tilde{g}(Z)$ are finite in that region (at least when L_{max} is finite). As shown in Figure 4b, the path of integration C comprises four pieces: C_2 and C_4 run from $-\infty$ to 0 a distance ϵ above and below the negative real axis respectively, C_3 is a semicircle of radius ϵ about the origin, and C_1 is (almost) a circle whose radius should be taken to infinity. For large Z we have from (3.16),

$$\frac{\tilde{g}'(Z)}{\tilde{g}(Z)} \xrightarrow{Z \rightarrow \infty} \frac{-D2^{D-1}\pi^{\frac{D}{2}-1}\Gamma(D/2)}{2a} b_0 Z^{-\frac{D}{2}-1} + \dots, \quad (3.34)$$

and it follows that

$$\int_{C_1} \frac{\tilde{g}'(Z)}{\tilde{g}(Z)} dZ = 0. \quad (3.35)$$

(We remind the reader of our standing assumption that $a \neq 0$. See the remarks following (3.19).) On the other hand the IR behaviour, $\tilde{g}(Z) \xrightarrow{Z \rightarrow 0} -Z$, leads to

$$\int_{C_3} \frac{\tilde{g}'(Z)}{\tilde{g}(Z)} dZ = i\pi. \quad (3.36)$$

Also, because $\tilde{g}(x + i\epsilon) = \overline{\tilde{g}(x - i\epsilon)}$ for $x < 0$:

$$\int_{C_2+C_4} \frac{\tilde{g}'(Z)}{\tilde{g}(Z)} dZ = 2i \int_{C_2} \text{Im} \left[\frac{\tilde{g}'(Z)}{\tilde{g}(Z)} \right] dZ. \quad (3.37)$$

Performing this last integral will allow us to determine whether $\square_\rho^{(D)}$ has unstable modes or not.

Given a choice of the parameters a and b_n , the last integral can be computed numerically. In the minimal 4D case discussed in Section 2.2, we find that $\square_\rho^{(4)}$ has precisely two “unstable zeros”. (Notice that because $\tilde{g}(\bar{Z}) = \overline{\tilde{g}(Z)}$, if Z is a zero of $\tilde{g}(Z)$, so also is \bar{Z} .) We have located these zeros numerically, as shown in Figure 3a. With different choices of the parameters $\{a, b_n\}$, the number of zeros can change, but we have not been able to find any choice that would make $\square_\rho^{(4)}$ stable. It would be interesting to find an analytical method to check for stability.

4 Summary and Remarks

We have defined an infinite family of scalar-field operators on causal sets which we dubbed Generalized Causet Box (GCB) operators. For causal sets made by sprinkling D -dimensional Minkowski space \mathbb{M}^D , these operators reproduce the usual d’Alembertian $\square = \nabla_\mu \nabla^\mu$ when one averages over all sprinklings and takes the limit of infinite sprinkling-density ρ . If, on the other hand, one averages over all sprinklings while holding ρ fixed, one obtains an integral operator $\square_\rho^{(D)}$ in \mathbb{M}^D which is manifestly Lorentz-invariant, retarded, and nonlocal, with the degree of nonlocality set by ρ . In the present paper, we have been concerned primarily with these continuum operators, whose nonlocality can be regarded as a “mesoscopic” residue of the underlying causal set discreteness.

The GCB operators $B_\rho^{(D)}$ and their continuum averages $\square_\rho^{(D)}$ are parametrized by a set of coefficients, and we derived the equations in these coefficients which ensure that \square is recovered in the infrared limit. The minimal solutions of these equations turned out to reproduce the original operators proposed in [2]. We also computed the Fourier transform of $\square_\rho^{(D)}$, or equivalently its “spectrum of eigenvalues” obtained by applying it to an arbitrary plane wave. For spacelike momenta the spectrum is real. For timelike momenta it contains also an imaginary part, which changes sign under interchange of past with future. The UV behaviour of the spectrum differs from that of \square in a way which led us to propose a genuinely Lorentzian, perturbative regulator for quantum field theory.

We also studied the question of whether the evolution defined by the continuum-averaged GCB operators is stable. This is of interest in relation to nonlocal field theories based on $\square_\rho^{(D)}$; it can also serve as an indicator of the stability or instability of the corresponding causet operator $B_\rho^{(D)}$. The continuum-average of the minimal 2D causal set d’Alembertian was shown to be stable by a direct proof. In 4D we did not settle the question analytically, but we devised a numerical diagnostic that applies to all the operators $\square_\rho^{(D)}$, and which disclosed a pair of unstable modes when applied to the minimal 4D causal set d’Alembertian. Are any of the continuum-averaged GCB operators stable in $3 + 1$ dimensions? We were not able to find any, but there are an infinite number of such operators

and a definitive search could only be conducted by analytical means.⁷ Finally, it bears repeating that there might be more reliable indicators of instability than simply the existence of an exponentially growing plane-wave solution, which a priori tells us nothing about the behavior of solutions of limited spatial extent. For that reason, it would be worthwhile to analyze directly the late-time behavior of the Green function $G_R(x - y)$ which is inverse to $\square_\rho^{(D)}$. If it were bounded that would imply stability, and if it grew exponentially, that would imply instability.

Our results also suggest other problems for further work. It would be interesting, for example, to work out the continuum-averaged GCB operators in curved spacetimes. It was found in [3] that the minimal 4D operator has the following limit as $\rho \rightarrow \infty$: $\square_\rho^{(4)} \Phi \rightarrow \square \Phi - \frac{1}{2} R \Phi$, where R is the Ricci scalar. (In fact one obtains the same limit in all dimensions D .) Would this feature persist for all of the GCB operators? This feature has also been used to define an action-functional for causal sets [3]. A final question then is whether the instability found above has any consequences for this causal set action?

Acknowledgments

We thank Niayesh Afshordi for useful discussions throughout the course of this project.

This research was supported in part by NSERC through grant RGPIN-418709-2012. This research was supported in part by Perimeter Institute for Theoretical Physics. Research at Perimeter Institute is supported by the Government of Canada through Industry Canada and by the Province of Ontario through the Ministry of Research and Innovation.

References

- [1] L. Bombelli, J. Lee, D. Meyer, and R. D. Sorkin, *Space-time as a causal set*, *Physical Review Letters* **59** (Aug., 1987) 521–524.
- [2] R. D. Sorkin, *Does Locality Fail at Intermediate Length-Scales*, in *Approaches to Quantum Gravity – Towards a new understanding of space and time*, edited by Daniele Oriti, Cambridge University Press (2009) 26–43, [[gr-qc/0703099](#)].
- [3] D. M. T. Benincasa and F. Dowker, *Scalar Curvature of a Causal Set*, *Physical Review Letters* **104** (May, 2010) 181301, [[arXiv:1001.2725](#)].
- [4] F. Dowker and L. Glaser, *Causal set d’Alembertians for various dimensions*, *ArXiv e-prints* (May, 2013) [[arXiv:1305.2588](#)].
- [5] F. W. Olver, D. W. Lozier, R. F. Boisvert, and C. W. Clark, *NIST Handbook of Mathematical Functions*. Cambridge University Press, New York, NY, USA, 1st ed., 2010.
- [6] A. G. Domínguez and S. E. Trione, *On the laplace transforms of retarded, lorentz-invariant functions*, *Advances in Mathematics* **31** (1979), no. 1 51 – 62.

⁷Also interesting would be an unstable operator whose corresponding growth-time was either very large (cosmological) or very small (Planckian). In the former case, the instability would be irrelevant physically, in the latter case it might still be compatible with stability of the corresponding discrete evolution. We were not able to find any such operator in 4D either.

A IR Behaviour of the GCB Operators: Details

Here we will derive the equations that the constants a and $\{b_n\}$ should satisfy in order for $\square_\rho^{(D)}$ to have the desired IR behaviour (3.12), or equivalently (3.13), which in turn is equivalent to

$$\tilde{g}(Z) \xrightarrow{Z \rightarrow 0} -Z, \quad (\text{A.1})$$

where $\tilde{g}(Z)$ is defined by

$$\rho^{-2/D} g_\rho^{(D)}(p) \equiv \tilde{g}(Z), \quad (\text{A.2})$$

as given in the right hand side of (3.8).

A.1 Even Dimensions

Let $D = 2N + 2$ where $N = 0, 1, 2, \dots$. Then

$$\tilde{g}(Z) = a + 2(2\pi)^N \sum_{n=0}^{L_{max}} \frac{b_n}{n!} C_D^n \int_0^\infty s^{2(N+1)n+2N+1} e^{-C_D s^D} (Z^{1/2}s)^{-N} K_N(Z^{1/2}s) ds. \quad (\text{A.3})$$

In order to examine the behaviour of $\tilde{g}(Z)$ as $Z \rightarrow 0$, we need to expand $(Z^{1/2}s)^{-N} K_N(Z^{1/2}s)$ in this regime. From the power series expansion of K_N (see e.g. 10.31.1 and 10.25.2 of [5]), it follows that

$$(Z^{1/2}s)^{-N} K_N(Z^{1/2}s) = 2^{N-1} (Zs^2)^{-N} \sum_{k=0}^{N-1} \frac{\Gamma(N-k)}{k!} (-Zs^2/4)^k \quad (\text{A.4a})$$

$$+ \frac{(-1)^{N+1}}{2^{N+1}N!} \ln(Z) \quad (\text{A.4b})$$

$$+ \frac{(-1)^N}{2^{N+1}N!} [-2\ln(s/2) + \psi(1) + \psi(N+1)] \quad (\text{A.4c})$$

$$+ \frac{(-1)^{N+1}s^2}{2^{N+3}(N+1)!} Z \ln(Z) \quad (\text{A.4d})$$

$$+ \frac{(-1)^N}{2^{N+3}(N+1)!} [-2\ln(s/2) + \psi(2) + \psi(N+2)] s^2 Z \quad (\text{A.4e})$$

$$+ \mathcal{O}(Z^2),$$

where $\psi(n)$ is the digamma function. Because we need the leading behaviour of $\rho^{-\frac{2}{D}} \tilde{g}(Z)$ to be $-Z$, we have only considered terms up to this order. All the terms in (A.4a) and (A.4b) diverge as $Z \rightarrow 0$, forcing us to pick the b_n such that none of them contribute to $\tilde{g}(Z)$ in the $Z \rightarrow 0$ limit. The contribution of the term (A.4d) is also unwanted and should be made to vanish by choosing b_n appropriately. This leads us to the following series of equations:

$$\sum_{n=0}^{L_{max}} \frac{b_n}{n!} C_D^n \int_0^\infty s^{2(N+1)n+2k+1} e^{-C_D s^D} ds = 0, \quad k = 0, 1, \dots, N+1. \quad (\text{A.5})$$

The integration over s can be performed (see e.g. 5.9.1 of [5]) to give us the condition reproduced above as equation (3.14a):

$$\sum_{n=0}^{L_{max}} \frac{b_n}{n!} \Gamma(n + \frac{k+1}{N+1}) = 0, \quad k = 0, 1, \dots, N+1. \quad (\text{A.6})$$

Requiring the contribution of the constant term (A.4c) to vanish yields

$$a + \frac{(-1)^{N+1} 2\pi^N}{N!} \sum_{n=0}^{L_{max}} \frac{b_n}{n!} C_D^n \int_0^\infty s^{2(N+1)n+2N+1} e^{-C_D s^D} \ln(s) ds = 0. \quad (\text{A.7})$$

We can perform the integral over s by using the formula (see e.g. 5.9.19 and 5.9.1 of [5])

$$\int_0^\infty s^\mu e^{-as^D} \ln(s) ds = \frac{\Gamma(\frac{\mu+1}{D})}{D^2 a^{\frac{\mu+1}{D}}} \left[\psi(\frac{\mu+1}{D}) - \ln(a) \right], \quad (\text{A.8})$$

leading to (3.14b):

$$a + \frac{2(-1)^{N+1} \pi^N}{D^2 C_D N!} \sum_{n=0}^{L_{max}} b_n \psi(n+1) = 0. \quad (\text{A.9})$$

Finally, requiring the contribution of (A.4e) to reproduce the desired $-Z$ behaviour leads to

$$\sum_{n=0}^{L_{max}} \frac{b_n}{n!} C_D^n \int_0^\infty s^{2(N+1)n+2N+3} e^{-C_D s^D} \ln(s) ds = \frac{2(-1)^N (N+1)!}{\pi^N}. \quad (\text{A.10})$$

Performing the integral using (A.8) furnishes (3.14c):

$$\sum_{n=0}^{L_{max}} \frac{b_n}{n!} \Gamma(n + \frac{N+2}{N+1}) \psi(n + \frac{N+2}{N+1}) = \frac{2(-1)^N (N+1)!}{\pi^N} D^2 C_D^{\frac{N+2}{N+1}}. \quad (\text{A.11})$$

A.2 Odd Dimensions

Let $D = 2N + 1$ where $N = 0, 1, 2, \dots$. Then

$$\tilde{g}(Z) = a + 2(2\pi)^{N-1/2} \sum_{n=0}^{L_{max}} \frac{b_n}{n!} C_D^n \int_0^\infty s^{2(N+1)n+2N} e^{-C_D s^D} (Z^{1/2} s)^{-N+1/2} K_{N-1/2}(Z^{1/2} s) ds. \quad (\text{A.12})$$

From the power series expansion of K_N (see 10.27.4 of and 10.25.2 of [5]), it follows that

$$(Z^{\frac{1}{2}} s)^{-N+\frac{1}{2}} K_{N-\frac{1}{2}}(Z^{\frac{1}{2}} s) = (-1)^{N-1} 2^{N-\frac{3}{2}} \pi (Z^{\frac{1}{2}} s)^{-2N+1} \sum_{k=0}^N \frac{(Z s^2/4)^k}{k! \Gamma(k - N + \frac{3}{2})} \quad (\text{A.13a})$$

$$+ \frac{(-1)^N 2^{-N-\frac{1}{2}} \pi}{\Gamma(N + \frac{1}{2})} \quad (\text{A.13b})$$

$$+ \frac{(-1)^N 2^{-N-\frac{5}{2}} \pi}{\Gamma(N + \frac{3}{2})} s^2 Z \quad (\text{A.13c})$$

$$+ \mathcal{O}(Z^{3/2}).$$

As before, we have only kept track of terms up to Z . The contributions of all the terms in (A.13a) should be made to vanish; this leads to the equation

$$\sum_{n=0}^{L_{max}} \frac{b_n}{n!} C_D^n \int_0^\infty s^{2(N+1)n+2k+1} e^{-C_D s^D} ds = 0, \quad k = 0, 1, \dots, N. \quad (\text{A.14})$$

Performing the integral over s gives us (3.15a):

$$\sum_{n=0}^{L_{max}} \frac{b_n}{n!} \Gamma(n + \frac{2k+2}{2N+1}) = 0, \quad k = 0, 1, \dots, N. \quad (\text{A.15})$$

Requiring the contribution of the constant term (A.13b) to vanish yields

$$a + \frac{(-1)^N \pi^{N+\frac{1}{2}}}{\Gamma(N + \frac{1}{2})} \sum_{n=0}^{L_{max}} \frac{b_n}{n!} C_D^n \int_0^\infty s^{2(N+1)n+2N} e^{-C_D s^D} ds = 0, \quad (\text{A.16})$$

which is equivalent to (3.15b):

$$a + \frac{(-1)^N \pi^{N+\frac{1}{2}}}{DC_D \Gamma(N + \frac{1}{2})} \sum_{n=0}^{L_{max}} b_n = 0. \quad (\text{A.17})$$

Finally, requiring the contribution of (A.13c) to reproduce the desired $-Z$ behaviour leads to

$$\frac{(-1)^N \pi^{N+\frac{1}{2}}}{4\Gamma(N + \frac{3}{2})} \sum_{n=0}^{L_{max}} \frac{b_n}{n!} C_D^n \int_0^\infty s^{2(N+1)n+2N+2} e^{-C_D s^D} ds = -1, \quad (\text{A.18})$$

which furnishes (3.15c):

$$\sum_{n=0}^{L_{max}} \frac{b_n}{n!} \Gamma(n + \frac{2N+3}{2N+1}) = \frac{(-1)^{N-1} 4\Gamma(N + \frac{3}{2})}{\pi^{N+\frac{1}{2}}} DC_D^{\frac{2N+3}{2N+1}}. \quad (\text{A.19})$$

B UV Behaviour of the GCB Operators: Details

Here we derive the UV behaviour of $\square_\rho^{(D)}$. We will make use of the following identity [6], which holds for arbitrary natural number m :

$$\frac{K_p(Z^{\frac{1}{2}} s)}{Z^{\frac{p}{2}}} = (-1)^m \left(\frac{2}{s}\right)^m \frac{d^m}{dZ^m} \left\{ \frac{K_{p-m}(Z^{\frac{1}{2}} s)}{Z^{\frac{p-m}{2}}} \right\}. \quad (\text{B.1})$$

B.1 Even Dimensions

Let $D = 2N + 2$ where $N = 0, 1, 2, \dots$, and $p = m = N$ in (B.1). It then follows that

$$Z^{-N/2} K_N(Z^{\frac{1}{2}} s) = (-1)^N \left(\frac{2}{s}\right)^N \frac{d^N}{dZ^N} K_0(Z^{\frac{1}{2}} s). \quad (\text{B.2})$$

Substituting this in the definition of $\tilde{g}(Z)$, as given by (A.3), produces

$$\tilde{g}(Z) = a + (-1)^N 2^{2N+1} \pi^N \sum_{n=0}^{L_{max}} \frac{b_n}{n!} C_D^n \frac{d^N}{dZ^N} I_n^{(D)}(Z), \quad (\text{B.3})$$

where

$$I_n^{(D)}(Z) \equiv \int_0^\infty s^{Dn+1} e^{-C_D s^D} K_0(Z^{\frac{1}{2}} s) ds. \quad (\text{B.4})$$

It then suffices to study the behaviour of this integral as $Z \rightarrow \infty$. It follows from 10.29.4 of [5] that

$$K_0(Z^{\frac{1}{2}} s) = \frac{-1}{Z^{\frac{1}{2}} s} \frac{d}{ds} \left(s K_1(Z^{\frac{1}{2}} s) \right). \quad (\text{B.5})$$

Plugging this relation in (B.4) and integrating by parts yields

$$I_n^{(D)}(Z) = -\frac{1}{Z^{\frac{1}{2}}} \left\{ s^{Dn+1} e^{-C_D s^D} K_1(Z^{\frac{1}{2}} s) \Big|_0^\infty - \int_0^\infty s K_1(Z^{\frac{1}{2}} s) \frac{d}{ds} (s^{Dn} e^{-C_D s^D}) ds \right\}. \quad (\text{B.6})$$

The first term vanishes when evaluated at ∞ . When evaluated at 0, it is non-zero only when $n = 0$, because $K_1(Z^{\frac{1}{2}} s) \rightarrow Z^{\frac{1}{2}} s^{-1}$ when $s \rightarrow 0$. It then follows that

$$I_n^{(D)}(Z) = \frac{1}{Z^{\frac{1}{2}}} \left\{ \frac{\delta_{n0}}{Z^{\frac{1}{2}}} + \int_0^\infty s K_1(Z^{\frac{1}{2}} s) \frac{d}{ds} (s^{Dn} e^{-C_D s^D}) ds \right\}. \quad (\text{B.7})$$

From 10.29.3 of [5],

$$K_1(Z^{\frac{1}{2}} s) = \frac{-1}{Z^{\frac{1}{2}} s} \frac{d}{ds} K_0(Z^{\frac{1}{2}} s). \quad (\text{B.8})$$

Plugging this back into (B.7) and integrating once again by parts yields

$$I_n^{(D)}(Z) = \frac{1}{Z} \left\{ \delta_{n0} + \int_0^\infty K_0(Z^{\frac{1}{2}} s) \frac{d}{ds} \left[s \frac{d}{ds} (s^{Dn} e^{-C_D s^D}) \right] ds \right\}. \quad (\text{B.9})$$

It can be shown that

$$\lim_{Z \rightarrow \infty} \int_0^\infty K_0(Z^{\frac{1}{2}} s) \frac{d}{ds} \left[s \frac{d}{ds} (s^{Dn} e^{-C_D s^D}) \right] ds = 0. \quad (\text{B.10})$$

With the aid of (B.3), it then follows that for large Z ,

$$\tilde{g}(Z) = a + 2^{D-1} \pi^{\frac{D}{2}-1} \Gamma(D/2) b_0 Z^{-\frac{D}{2}} + \dots \quad (\text{B.11})$$

Notice that both these terms are real for both positive and negative Z , because $D/2$ is an integer when D is even. In order to produce the sub-leading terms, one can continue integrating by parts in (B.9). The sub-leading terms are thus also real, whence the imaginary part of $\tilde{g}(Z)$ must, for even D , decay faster than any power of Z for $Z \rightarrow \infty$. This behavior can be seen in Figures 2b and 3b.

B.2 Odd Dimensions

Let $D = 2N + 1$ where $N = 0, 1, 2, \dots$, and $p = m - \frac{1}{2} = N - \frac{1}{2}$ in (B.1). It then follows that

$$Z^{\frac{1-2N}{4}} K_{N-\frac{1}{2}}(Z^{\frac{1}{2}} s) = (-1)^N \left(\frac{2}{s} \right)^N \frac{d^N}{dZ^N} \{ Z^{\frac{1}{4}} K_{-\frac{1}{2}}(Z^{\frac{1}{2}} s) \}. \quad (\text{B.12})$$

From 10.39.2 of [5], we have that

$$K_{-\frac{1}{2}}(Z^{\frac{1}{2}} s) = Z^{-\frac{1}{4}} \left(\frac{\pi}{2s} \right)^{\frac{1}{2}} e^{-Z^{\frac{1}{2}} s}, \quad (\text{B.13})$$

whence

$$Z^{\frac{1-2N}{4}} K_{N-\frac{1}{2}}(Z^{\frac{1}{2}}s) = \frac{(-1)^N 2^{N-\frac{1}{2}} \pi^{\frac{1}{2}}}{s^{N+\frac{1}{2}}} \frac{d^N}{dZ^N} e^{-Z^{\frac{1}{2}}s}. \quad (\text{B.14})$$

Substituting this into the definition of $\tilde{g}(Z)$, as given by (A.12), produces

$$\tilde{g}(Z) = a + (-1)^N 2^{2N} \pi^N \sum_{n=0}^{L_{max}} \frac{b_n}{n!} C_D^n \frac{d^N}{dZ^N} I_n^{(D)}(Z), \quad (\text{B.15})$$

where

$$I_n^{(D)}(Z) \equiv \int_0^\infty s^{Dn} e^{-C_D s^D} e^{-Z^{\frac{1}{2}}s} ds. \quad (\text{B.16})$$

It then suffices to study the behaviour of this integral as $Z \rightarrow \infty$:

$$\begin{aligned} I_n^{(D)}(Z) &= -Z^{-\frac{1}{2}} \int_0^\infty s^{Dn} e^{-C_D s^D} \frac{d}{ds} e^{-Z^{\frac{1}{2}}s} ds \\ &= -Z^{-\frac{1}{2}} \left\{ s^{Dn} e^{-C_D s^D} e^{-Z^{\frac{1}{2}}s} \Big|_0^\infty - \int_0^\infty e^{-Z^{\frac{1}{2}}s} \frac{d}{ds} (s^{Dn} e^{-C_D s^D}) \right\} \\ &= Z^{-\frac{1}{2}} \left\{ \delta_{n0} + \int_0^\infty e^{-Z^{\frac{1}{2}}s} \frac{d}{ds} (s^{Dn} e^{-C_D s^D}) \right\}. \end{aligned} \quad (\text{B.17})$$

Again, because

$$\lim_{Z \rightarrow \infty} \int_0^\infty e^{-Z^{\frac{1}{2}}s} \frac{d}{ds} (s^{Dn} e^{-C_D s^D}) = 0, \quad (\text{B.18})$$

we can deduce from (B.15) that

$$\tilde{g}(Z) = a + 2^{D-1} \pi^{\frac{D}{2}-1} \Gamma(D/2) b_0 Z^{-\frac{D}{2}} + \dots \quad (\text{B.19})$$

C Derivation of Equation (2.5)

From the general equations, (3.4) and (3.7), we have

$$\rho^{-1} g_\rho^{(2)}(p) = a^{(2)} + \rho \sum_{n=0}^2 \frac{(-1)^n \rho^n}{n!} b_n^{(2)} \frac{\partial^n}{\partial \rho^n} \chi(p, \rho), \quad (\text{C.1})$$

where $\{a^{(2)}, b_n^{(2)}\}$ are given in (2.2) and

$$\chi(p, \rho) = 2 \int_0^\infty s e^{-\rho s^2/2} K_0(\sqrt{p \cdot p} s) ds. \quad (\text{C.2})$$

From the relation (see e.g. 8.6.6 and 8.19.1 of [5]),

$$e^Z E_1(Z) = 2 \int_0^\infty e^{-t} K_0(\sqrt{2zt}) dt, \quad (\text{C.3})$$

it follows that

$$\chi(p, \rho) = \rho^{-1} e^{Z/2} E_1(Z/2), \quad Z = \rho^{-1} p \cdot p. \quad (\text{C.4})$$

Furthermore, using the identities (see e.g. 8.9.14 and 8.19.12 of [5]),

$$\frac{d}{dz} [e^z E_p(z)] = e^z E_p(z) \left(1 + \frac{p-1}{z}\right) - \frac{1}{z}, \quad (\text{C.5})$$

$$pE_{p+1}(z) + zE_p(z) = e^{-z}, \quad (\text{C.6})$$

it can be shown that

$$\rho^2 \frac{\partial \chi}{\partial \rho} = e^{Z/2} E_2(Z/2) - e^{Z/2} E_1(Z/2) \quad (\text{C.7})$$

$$\rho^3 \frac{\partial^2 \chi}{\partial \rho^2} = e^{Z/2} E_1(Z/2) [2 + Z/2] - e^{Z/2} E_2(Z/2) [3 + Z/2]. \quad (\text{C.8})$$

Equation (2.5) results from plugging these expressions back into (C.1) and using (C.6):

$$\rho^{-1} g_p^{(2)}(p) = -Z e^{Z/2} E_2(Z/2). \quad (\text{C.9})$$

D Damping the fluctuations

In reference [2] a prescription was given to get from the causet d'Alembertian $B_\rho^{(2)}$ of (2.1) a new operator $\tilde{B}_{\rho,\epsilon}^{(2)}$, whose fluctuations are damped, but which has the same mean over sprinklings as $B_{\tilde{\rho}}^{(2)}$ with $\tilde{\rho} = \epsilon\rho$. Here we generalize this prescription to the class of causet d'Alembertians $B_\rho^{(D)}$ defined in (3.1). (See Sections 2 and 3 for any symbol which is not defined in what follows.)

Given the causal set d'Alembertian,

$$\rho^{-2/D} (B_\rho^{(D)} \Phi)(x) = a\Phi(x) + \sum_{m=0}^{L_{max}} b_m \sum_{y \in I_m} \Phi(y), \quad (\text{D.1})$$

we construct as follows a new operator $\tilde{B}_{\rho,\epsilon}^{(D)}$ whose effective non-locality energy-density scale is $\epsilon\rho$:

$$\tilde{\rho}^{-2/D} (\tilde{B}_{\rho,\epsilon}^{(D)} \Phi)(x) = a\Phi(x) + \sum_{n=0}^{\infty} \tilde{b}_n \sum_{y \in I_n} \Phi(y), \quad (\text{D.2})$$

with

$$\tilde{b}_n = \epsilon(1-\epsilon)^n \sum_{m=0}^{L_{max}} \binom{n}{m} \frac{b_m \epsilon^m}{(1-\epsilon)^m}, \quad \epsilon = \tilde{\rho}/\rho. \quad (\text{D.3})$$

(Here, the binomial coefficient $\binom{n}{m}$ is zero by convention for $m > n$.)

Let us demonstrate that the continuum limit of $\tilde{B}_{\rho,\epsilon}^{(D)}$, which we will denote by $\tilde{\square}_{\tilde{\rho}}^{(D)}$, is equal to $\square_{\tilde{\rho}}^{(D)}$:

$$\begin{aligned}
& \tilde{\rho}^{-2/D} (\tilde{\square}_{\tilde{\rho}}^{(D)} \Phi)(x) - a\Phi(x) \\
&= \rho \sum_{n=0}^{\infty} \frac{\tilde{b}_n}{n!} \int_{J^-(x)} e^{-\rho V(x,y)} [\rho V(x,y)]^n \phi(y) dV_y \\
&= \rho \epsilon \sum_{m=0}^{L_{max}} \frac{b_m \epsilon^m}{m!} \int_{J^-(x)} e^{-\rho V(x,y)} \left\{ \sum_{n=m}^{\infty} \frac{(1-\epsilon)^{n-m}}{(n-m)!} [\rho V(x,y)]^n \right\} \phi(y) dV_y \\
&= \tilde{\rho} \sum_{m=0}^{L_{max}} \frac{b_m}{m!} \int_{J^-(x)} e^{-\rho V(x,y)} \left\{ \sum_{n=m}^{\infty} \frac{(1-\epsilon)^{n-m}}{(n-m)!} [\rho V(x,y)]^{n-m} \right\} [\epsilon \rho V(x,y)]^m \phi(y) dV_y \\
&= \tilde{\rho} \sum_{m=0}^{L_{max}} \frac{b_m}{m!} \int_{J^-(x)} e^{-\rho V(x,y)} e^{(1-\epsilon)\rho V(x,y)} [\tilde{\rho} V(x,y)]^m \phi(y) dV_y \\
&= \tilde{\rho} \sum_{m=0}^{L_{max}} \frac{b_m}{m!} \int_{J^-(x)} e^{-\tilde{\rho} V(x,y)} [\tilde{\rho} V(x,y)]^m \phi(y) dV_y. \\
&= \tilde{\rho}^{-2/D} (\square_{\tilde{\rho}}^{(D)} \Phi)(x) - a\Phi(x).
\end{aligned}$$

Of course, we have not proven here that the fluctuations of $\tilde{B}_{\tilde{\rho}}^{(D)}$ are actually damped. This has been confirmed numerically for the minimal 2D and 4D operators in [2] and [3]. It would be interesting to confirm it also for the full set of GCB operators in all dimensions.